On the transition to gasoline-to-olefins chemistry in the cracking reactions of 1-octene over H-ZSM-5 catalysts

Alexander P. Hawkins [a,1], Andrea Zachariou [a,2], Stewart F. Parker [a,b,*], Paul Collier [c], Nathan S. Barrow [c], Russell F. Howe [d], David Lennon [a]

[a] School of Chemistry, Joseph Black Building, University of Glasgow, Glasgow G12 8QQ, UK
[b] ISIS Neutron and Muon Source, STFC Rutherford Appleton Laboratory, Oxon OX11 0QX, UK
[c] Johnson Matthey Technology Centre, Blounts Court, Sonning Common, Reading RG4 9NH, UK
[d] Department of Chemistry, University of Aberdeen, Aberdeen AB24 3UE, UK

ARTICLE INFO

ABSTRACT

The cracking reactions of 1-octene over H-ZSM-5 zeolite are studied via micro-reactor and off-line spectroscopic techniques for up to 72 h on stream and a temperature range of 473–673 K. 1-Octene is found to react *via* a two-cycle hydrocarbon pool mechanism, with strong similarities to that reported for methanol-to-hydrocarbons chemistry. This dual-cycle mechanism requires temperatures of 673 K or higher to function with full efficiency, with lower temperatures deactivating portions of the cyclic mechanism, leading to premature deactivation of the catalyst through over-production of coke species. Inelastic neutron scattering is used to study the coke composition, identifying two distinct deactivation mechanisms depending on reaction temperature. The catalyst is also found to slowly progress from an aromatic-heavy to an olefin-heavy product regime even at full efficiency due to progressive blockage of active sites by amorphous carbon-rich coke. Artificial aging of the zeolite, through steam treatment, is found to shift the catalyst lifetime so that it commences at a later stage in this process, resulting in increased light olefin production. The reduced aromatic production also means that deactivation of the catalyst occurs more slowly in steamed catalysts than in fresh ones, after an equivalent time-on-stream. Collectively, these observations connect with the application of ZSM-5 catalysts to facilitate gasoline-to-olefins chemistry in fluidised catalytic cracking unit operations.

1. Introduction

Fluidised catalytic cracking (FCC) reactions using acid zeolites are an important source of high-value hydrocarbons, being able to convert less commercially important heavy hydrocarbon fractions into more widely utilised feedstock chemicals [1–3]. The selectivity of zeolite catalysed reactions arises from shape-selective effects due to the microporous structure of the catalyst. H-ZSM-5 zeolites are widely used due to their MFI-type structure leading to an ability to convert gasoline-range hydrocarbons to light olefins such as ethene and propene with high yield [4–7]. In this application, the hydrocarbon fraction which is active for conversion by H-ZSM-5 is the straight and branched olefins in the C_7-C_{12} size range [6]. 1-Octene is therefore frequently used as a model compound to allow the study of this type of cracking chemistry under controlled conditions [8–10].

The primary mechanism behind the increased propene production by ZSM-5 is considered to be a transition state shape-selective effect [6]. Cracking reactions of olefins over zeolite catalysts are thought to occur *via* protonation of the double bond by Brønsted sites to form a bound carbenium ion. This ion may then undergo either a bimolecular reaction involving the addition of another olefin followed by further isomerisation and hydrogen transfer steps, or monomolecular cracking reactions proceeding through either β-scission or protonated cyclopropane intermediates [6,11]. In ZSM-5, due to the restricted pore diameter, olefins larger than C4 have insufficient space to react via the bimolecular mechanism; an effect made more significant because the hydrogen transfer reactions which play an important role in the further steps in this reaction pathway require the participation of yet further reactant

---

molecules as hydride donors or acceptors. Therefore, larger FCC reactants react exclusively through the monomolecular mechanisms involving scission, resulting in a higher production of small molecules such as light olefins. This effect is magnified by the fact that in the β-scission mechanism the post-scission primary carbocation may be stabilised by one of two routes: an isomerisation to a secondary carbocation, optionally followed by a desorption of that carbocation as a disubstituted olefin or by a further bond cleavage resulting in release as two separate, smaller olefin molecules. Under ordinary conditions, it is the isomerisation pathway which is energetically favoured. However, in ZSM-5 the dimensions of the pores mean that the interactions between the closely located framework oxygens and the carbocation act to stabilise the intermediates in the bond cleavage mechanism, further driving the product balance toward the smaller olefins [6].

Acidity and mesoporosity are critical properties of the zeolite but these parameters that are by no means constant throughout the lifetime of the catalyst. For instance, hydrothermal conditions in catalytic use result in partial de-alumination of the zeolite framework at a rate determined by both the reactor temperature and the concentration of aluminium substitutions within the zeolite [11]. (The partial pressure of steam within the reactor also affects the rate of aluminium loss, but the magnitude of this effect is considerably less than the effects of temperature or zeolite composition [12]). This leads to a corresponding reduction in the number of acid sites, since removing an aluminium atom also removes its associated Brønsted O-H acid group, and possible increases in mesoporosity depending on the aluminium level of the zeolite and what proportion of the framework is removed [11,13]. Effects of this loss of acidity can be dramatic, with numerous studies reporting improved selectivity, stability and even activity in steamed zeolites relative to studies performed using fresh materials [14–16]. Most notably for FCC applications, H-ZSM-5 cracking catalysts are reported as being briefly able to catalyse the cracking of paraffins at the start of their time on-stream, a reactivity which is not observed during steady-state operation and which is attributed to the higher acidity of the unreacted catalyst [6].

Changes due to de-alumination from catalytic use can be simulated by the steam treatment of fresh zeolite allowing the generation of model zeolite materials whose properties closely match those of used or partially-deactivated catalysts [11,13,17]. Since the rate of de-alumination is proportional to aluminium concentration [11], an operating catalyst will spend the majority of its lifetime with a pseudo steady-state level of acidity because the rate of further aluminium loss is low, and such steamed catalysts may therefore be viewed as representative of a cracking catalyst in the middle or near the end of its operational lifetime.

The effect of steaming on ZSM-5 has been extensively studied [18–22]. There is general agreement that removal of framework aluminium has several effects beyond a simple reduction in the number of acid sites. These may include changes in both the strength and distribution of the acid sites by the selective removal of a particular fraction of Al atoms from specific framework positions and formation of additional mesopores and amorphous deposits that can be removed by post-treatment acid washing. The intensity of steaming is a crucial factor. Short, mild steaming leads to surface mesoporosity and the formation of strong acid sites due to the interaction with extra-framework species. It may also result in the re-insertion of Al into the framework resulting in increased total concentration of acid sites. Harsh steaming results in a more uniform distribution of mesopores and a drastic reduction in the number of Brønsted acid sites. It is noteworthy that inequivalent framework Al-sites are affected differently.

This study describes the preparation and characterisation of an extensively steamed ZSM-5 zeolite catalyst and directly compares its catalytic activity for the conversion of 1-octene with that of the untreated fresh zeolite across a range of different reaction regimes determined by temperature. Both the products released during the reaction and the retained coke species within the zeolite are characterised,

allowing investigation of the reaction mechanisms and deactivation pathways. Adding breadth to the study, the technique of inelastic neutron scattering (INS) is employed to provide information on the molecularity of species retained within the zeolite's porous network as a function of sample history. Thus, the article examines the reactivity and product selectivity of a ZSM-5 catalyst over a range of conditions relevant to FCC process operations.

It is recognised that our experimental conditions (473, 573 and 673 K, catalyst to reactant ratio $\gg$ 1, contact time 10 s of seconds) are distinctly different to those that are used industrially [1] (773–823 K, catalyst-to-reactant ratio $\sim$ 1, contact time 2–4 s). However, the product slate is very similar to the industrial system; hence, we believe that the compromises needed for a laboratory-scale investigation mean that the results are still relevant industrially.

2. Experimental

The ZSM-5 used, henceforth referred to as the catalyst, was a powder form commercial material grade H-ZSM-5 zeolite supplied by Johnson Matthey and calcined in air for 12 h at 773 K to remove the residual synthesis template. Characterisation of this catalyst showed it to possess a framework Si:Al ratio of 30:1, established by solid state ^{27}Al and ^{29}Si NMR. Previous investigations using the same catalyst have shown it to possess an average crystallite size of 0.1 × 0.1 × 0.5 μm: [23] the calcined catalyst was also sieved to provide consistent crystallite agglomerate sizes in the 200–500 μm range. Use of this unmodified catalyst in further experiments and tests will be identified as ZSM5-FR, with FR signifying 'fresh' catalyst.

2.1. Zeolite steam treatment

To prepare the artificially aged zeolite, 30 g of zeolite were steamed according to the following procedure: the sample was heated in a flowing gas comprising 10 % steam in air and ramped at 10 °C/min with the steam introduced above 200 °C. The sample was held at 800 °C for 12 h then cooled to 200 °C when the steam was stopped before cooling to room temperature. The resulting de-aluminated catalyst is designated ZSM5-ST, with ST signifying 'steamed' catalyst.

2.2. Zeolite characterisation

Characterisation measurements of both ZSM5-FR and ZSM5-ST were carried out to assess the effects of the steam treatment. The degree of framework de-alumination in ZSM5-ST was determined by comparing the results of ^{27}Al NMR. Acquisition took place in a static magnetic field strength of 9.4 T ($\nu_0(^1H)$ = 400 MHz) on a Bruker Avance III console using TopSpin 3.5 software. A wide-bore Bruker 4 mm MAS probe was used, tuned to 104.27 MHz and referenced to yttrium aluminium garnet at 0.0 ppm. Samples for measurement were left in a humid environment overnight and packed into zirconia MAS rotors with Kel-F caps. Before and after weight measurements provided the sample mass for normalisation. The rotors were spun at 14 kHz using room-temperature purified compressed air. Nutation tip angle was 22.5° and the relaxation time was 0.1 s, 8192 scans were acquired using a one pulse acquisition programme.

To quantify the acidity of both samples, ammonia temperature-programmed desorption (TPD) experiments were carried out using a Quantachrome ChemBET Pulsar instrument equipped with a thermal conductivity detector. Samples were dried at 623 K under flowing helium (15 cm^3 min^{-1}, BOC, >99.999 %) then cooled to 373 K and saturated with ammonia by passing 10 % NH$_3$ in He (15 cm^3 min^{-1}) through the sample for 15 min. The sample was returned to helium flow and purged for 2 h at the same temperature; these conditions are reported to remove any physisorbed ammonia from the zeolite pore network leaving only molecules chemisorbed to silanol groups, Lewis silanol or Brønsted acid sites [24]. Desorption was then carried out from 373 to 973 K with a

heating rate of 5 K min^{-1} and a 30 min hold at the highest temperature to ensure full removal of all ammonia.

Surface area analysis was performed using a Quantachrome Quadrasorb EVO/SI gas adsorption instrument. 0.15 g samples of the zeolites were degassed to < 20 mTorr at 523 K and gas adsorption and desorption isotherms were collected across a relative pressure (P/P$_0$) range from $5 \times 10^{-4} - 0.99$ using liquid nitrogen as the coolant and N$_2$ as the adsorbant gas. Isotherm analysis was carried out by the method of Brunauer, Emmett and Teller using software supplied with the instrument [25]. Sample microporosity levels were estimated using the *t*-plot method of de Boer [26]. The experiment was repeated three times for each material, with the mean and standard deviation values reported.

Powder X-ray diffraction measurements were carried out at room temperature with a Rigaku Miniflex 600 powder X-ray diffractometer.

2.3. Reaction testing

The 1-octene cracking reactions were carried out in a vertically oriented fixed-bed tube micro-reactor with an internal diameter of 10 mm; catalyst masses were approximately 0.5 g, giving a bed length of 10 mm. Samples were loaded into reactor tubes, purged with either He or N$_2$ (see below) and heated to the reaction temperature and held for 1 h prior to the commencement of the experiment to ensure the removal of any adsorbed atmospheric water. Reactions were performed at temperatures of 473, 573 and 673 K for both ZSM5-FR and ZSM5-ST. Exact catalyst masses and conditions for each reaction are given in Table S1 of the supplementary information section.

The reagent used was 1-octene (Sigma-Aldrich, 99 %), supplied at a rate calculated to give a weight-hourly space velocity (WHSV) of 1 h^{-1}. Octene injection was made using a syringe pump into a silica-packed mixing volume heated to 423 K and located immediately upstream of the reactor tube to ensure its complete vaporisation prior to entering the reactor. A 50 cm^3 min^{-1} flow of inert gas was used as a carrier for the 1-octene and any reaction products; this was helium (BOC, >99.999 %) for the initial two reactions (ZSM5-FR-673 K, ZSM5-ST-673 K), subsequent reactions used nitrogen (BOC, >99.999 %) for reasons of expense. The inlet pressure of the reactor was recorded; on commencement of the flow through the reactor it rose to 0.6 barg in all cases due to back-pressure from the catalyst bed but was not observed to vary significantly as the reactions progressed.

In order to provide on-line analysis of the reaction products the eluent gas flow from the reactor was analysed by both gas chromatography (GC) and mass spectrometry (MS). GC analysis was provided by a GC-FID (Shimadzu GC-2014 fitted with a BP20 column of dimensions 30 m x 0.25 mm × 0.5 μm) drawing from a 150 μl heated sample loop. MS analysis was provided by an ESS EcoCat drawing from immediately downstream of the GC sample loop using a differentially pumped heated capillary. All pipework between the reactor and the analysis instruments was maintained at 423 K to prevent condensation of any products within the pipework. Zero percent conversion data for each reaction was collected by initially bypassing the reactor for at least 30 min after the 1-octene injection was initiated. This also allowed the concentration of 1-octene in the gas stream to stabilise following pump breakthrough prior to starting the reaction. All reaction times are given from the commencement of flow through the reactor following these bypass measurements, this being t = 0 for each reaction. The target reaction period was 72 h on-stream for each reaction. However, the reactions at 473 K were terminated early after exhibiting no significant changes in product concentrations for an extended period after 12 h. Following completion of the reaction, the 1-octene flow was stopped and the reactor purged with continued inert gas flow for 30 min at reaction temperature to remove mobile products and residual 1-octene from the reactor. The on-line analysis was then stopped, gas flow through the reactor halted and the reactor allowed to cool to room temperature.

2.4. Post-reaction analysis

In order to determine the quantity of retained hydrocarbon species ('coke') within the catalysts post-reaction, samples of the reacted catalysts were subjected to thermogravimetric analysis (TGA) performed from 373 to 1000 K in a 10 % O$_2$ in N$_2$ gas flow using a TA Instruments TGA Q50 to oxidise the hydrocarbon fraction of the reacted samples. To determine the composition of these coke fractions, the catalysts were additionally analysed by Diffuse-Reflectance Infrared Fourier Transform Spectroscopy (DRIFTS) using an Agilent Carey 680 FTIR spectrometer equipped with a Harrick praying mantis beam accessory and heated sample cell with gas flow capability. Spectra were collected from 4000 to 1000 cm^{-1} using a liquid nitrogen cooled MCT detector with a resolution of 4 cm^{-1} and averaged over 64 scans per spectrum. Samples were purged with dry N$_2$ from a liquid nitrogen boil-off source (25 ml min^{-1}) then heated to 423 K at 5 K min^{-1} and held for 30 min under continued flow prior to prior to spectrum collection to ensure the removal of any adsorbed water collected during sample storage. This was considered unlikely to affect the composition of the hydrocarbons within the sample due to there having been purged at higher temperatures during the reactor shutdown process. Spectra of the clean, unreacted catalysts were also collected at this time for comparison purposes.

It was decided that greater insight into the coke species produced by the 573 K and 673 K reactions could be gained by analysing them using inelastic neutron scattering (INS) spectroscopy. To prepare samples of sufficient size for this technique, additional reactions at 573 K and 673 K were performed for both ZSM5-FR and ZSM5-ST at a scale of *ca.* 5 g$_{cat}$ using a large-scale catalyst preparation reactor located at the ISIS Neutron and Muon Source [27]. Total time-on-stream was 24 h for all reactions in this series. These larger samples were then investigated on the ISIS Facility's MAPS [28] and TOSCA [29] spectrometers; two instruments were used as each provides superior resolution in different regions of the vibrational spectrum from 200 to 4000 cm^{-1} [30].

An additional advantage of this repeated measurement was that the larger quantity of catalyst in these reactions allowed the collection of sufficient liquid products for infrared and gas chromatography-mass spectrometry (GC-MS) characterisation. Infrared spectra were collected using the attenuated total reflectance (ATR) method on a Nicolet iS10 instrument equipped with a Smart iTX diamond crystal ATR accessory and a deuterated triglycine sulphate detector. Spectra were collected from 4000^{-1} to 650 cm^{-1} at a resolution of 1 cm^{-1} and averaged over 64 scans per spectrum. GC-MS used an Agilent 7890 A gas chromatograph equipped with a series 5975 mass-selective detector. Component separation was achieved using a 60 m DB− 1MS nonpolar capillary column that achieved good separation of all product peaks.

3. Results

3.1. Zeolite characterisation

The zeolite characterisation measurements were performed to establish the differences in properties between the fresh, calcined catalyst (ZSM5-FR) and the steam treated, artificially aged material (ZSM5-ST). A summary of the results of these measurements is given in Table 1, with the associated profiles being reproduced in the supplementary information (Figs. S1-S3).

The reduction in the level of framework aluminium in ZSM5-ST resulting from the steam treatment is clearly illustrated by the results of the ^{27}Al NMR analysis (Table 1 and Fig. S1). In ZSM5-ST the peak at 53.4 ppm, representing the 4-coordinate AlO$_4$ environment of the aluminium T-atoms of the zeolite, is reduced to 26 % of its intensity in ZSM5-FR, indicating a corresponding removal of approximately three quarters of the framework aluminium by the steam treatment. The aluminium thus removed takes the form of a variety of extra-framework aluminium (EFAl) species, some of which are detectable by NMR.

Table 1

Zeolite parameters before and after steam treatment as established by ^{27}Al NMR and BET surface area analysis.

Sample:	^{27}Al NMR		Ammonia TPD:		BET Analysis:			
	Total Relative Intensity (± 0.03)	AlO$_4$ Relative Intensity (± 0.03)	Volume Adsorbed (μmol/g)	Population (sites/unit cell)	Micropore volume (cm^3/g)	Mesopore volume (cm^3/g)	External surface area (m^2/g)	Total Surface Area (m^2/g)
ZSM5-FR	1.00	0.91	366 ± 35	2.22 ± 0.21	0.101 ± 0.003	0.018 ± 0.001	50 ± 14	370 ± 11
ZSM5-ST	0.74	0.24	30 ± 5	0.18 ± 0.03	0.089 ± 0.005	0.037 ± 0.006	69 ± 14	332 ± 6

Evidence of both octahedral AlO$_6$ species at 1.4 ppm and partially removed framework aluminium around 30 ppm is observed, while the 26 % reduction in the overall intensity of the NMR spectrum indicates the formation of NMR-invisible polymeric aluminium clusters by a fraction of the EFAl. All of these observations are in line with the expected behaviour of ZSM-5 zeolites following steam treatment of the type used here [11,13,17,31,32].

The reduction in zeolite acidity resulting from this loss of framework aluminium is likewise extremely extensive. As shown in Fig. 1 the ν(O-H) peak for the Brønsted acid sites, located at 3605 cm^{-1} for the fresh zeolite, is essentially undetectable in the DRIFTS spectrum of ZSM5-ST. Despite this, ZSM5-ST does retain a small population of chemically active Brønsted sites (which may be hydrogen bonded to framework oxygen atoms). These can be detected by ammonia temperature-programmed desorption (TPD) analysis, indicated by the presence of chemisorbed ammonia which only desorbs at temperatures higher than 650 K, characteristic of bonding to Brønsted acid protons [24]. By comparison to the signal from known volumes of ammonia, the TPD measurements allow quantification of the number of acid sites per unit cell in each sample, which allows us to determine that ZSM5-ST possesses 8 % ± 2 % of the number of acid sites in ZSM5-FR (Fig. S2).

Even prior to steam treatment, the number of acid sites (and associated aluminium substitutions) per unit cell measured by ammonia TPD indicate that aluminium occupies only 3.4 % of the T-atom sites in ZSM5-FR, and their removal is therefore not expected to significantly affect the microporous structure of the zeolite framework. BET gas adsorption experiments using N$_2$ as the adsorbent gas (Fig. S3 top) show some degree of reduction in micropore volume, which can be attributed to the presence of EFAl species within the micropores. A small increase in mesoporosity induced by steaming is apparent (Table 1), however, the bulk structure is largely unchanged as shown by the close resemblance of the powder XRD spectra of the fresh and steamed zeolite (Fig. S3 bottom).

3.2. Reaction products analysis

Due to the large range of products from the 1-octene cracking

reaction resulting in extremely complex GC traces for the micro-reactor experiments, on-stream analysis of the reaction products used was accomplished by mass spectrometry as the primary method. It is therefore necessary to establish the fragmentation pattern of octene within the mass spectrometer to act as a baseline and the level of any potential thermal cracking, so that the effects of the acid and microporous catalysis of the ZSM-5 materials may be determined. To this end, blank reactions using ~1.5 g samples of amorphous silica in place of the ZSM-5 catalysts were run at 473, 573 and 673 K. After allowing the system to stabilise, this yielded the ion intensities presented in Fig. 2(i); the mass traces with time are reproduced in the supplementary information as Figs. S4-S6. The conditions were chosen to give the same bed
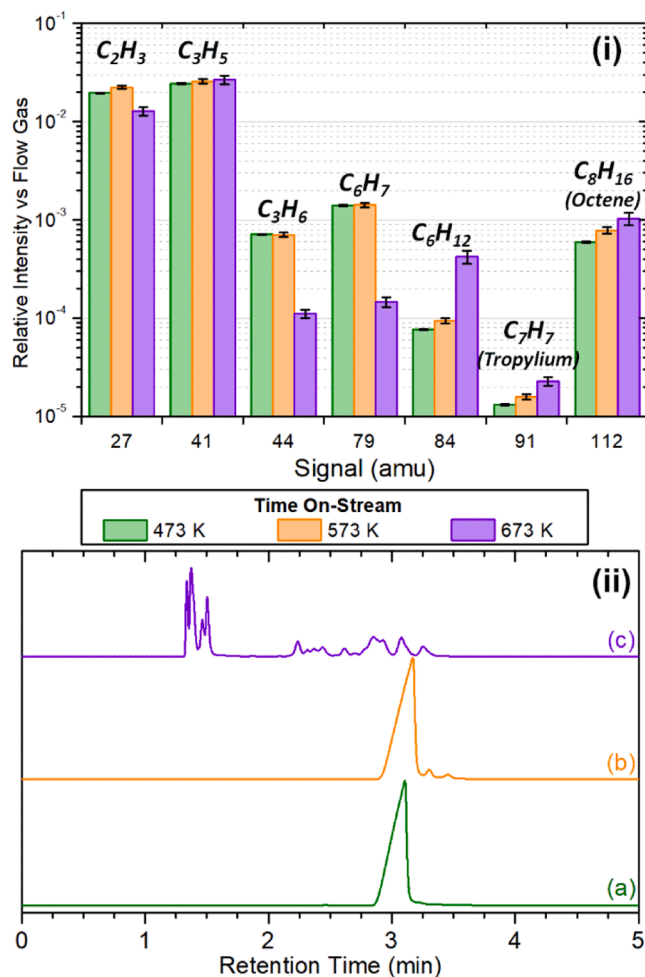
Fig. 2. Products from passing 1-octene over a SiO$_2$ blank at 473 K (a), 573 K (b) and 673 K (c) monitored by MS (i) and GC (ii). MS intensities normalised against the signal for the reaction flow gas (4 amu for He, 28 amu for N$_2$) to allow comparison between samples and averaged over the period + 01:00:00 to + 02:00:00 with errors shown. Labels over each bar group indicate ion fragment responsible for the majority of signal at each MS amu value. [1-Column].
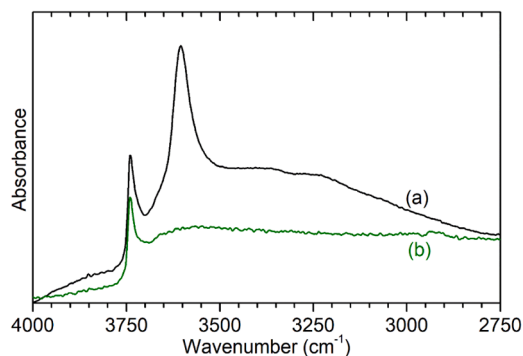

Fig. 1. Infrared spectra of ZSM5-FR (a) and ZSM5-ST (b). Spectra collected using DRIFTS and intensities normalised on the zeolite framework combination mode at 1870 cm^{-1} to allow direct comparison between the samples.

length and octene injection rate as in the catalytic reaction experiments.

The mass spectral profiles presented in Fig. 2(i) show that at 473 K the temperature is not high enough for any thermal cracking to occur, as no change in MS intensities were observed when the gas flow was switched from the bypass system to the reactor at t = 0. The resulting pattern is therefore due to fragmentation of 1-octene in the MS and is dominated by light species such as propyl and ethyl fragments (amu = 27, 41, 44). Hexyl fragments (amu 79) are also present, although their lower levels indicate that breakdown of the C_8 chain into $< C_4$ units is favoured. Importantly, the molecular octyl ion at 112 amu has sufficient intensity to allow its use in assessing the level of octene conversion in the actual reactions.

At 573 the fragmentation pattern is essentially the same as that observed at 473 K. In contrast, at 673 K Fig. 2(i) shows the mass spectrum to exhibit considerable reductions in the levels of larger alkyl ions, particularly hexyl fragments (79 amu), with increased signals for lighter fragments. Examination of the eluent by gas chromatography (Fig. 2(ii)) shows the suppression of the single 1-octene peak observed at 3 min retention time at lower temperatures in favour of multiple signals with lower retention times, confirming that thermal cracking is leading to fragmentation of 1-octene in the reactor into smaller, faster-diffusing species. Comparison of the intensity of the octene GC peak before and after t = 0 suggests that approximately 15 % of the octene exits the reactor at 673 K without having undergone thermal cracking in this instance, *i.e.* ~85 % conversion.

In all reactions studied, the majority of the changes in product composition with time occurred within the first 24 h on stream, with subsequent changes being the progress of trends established within this initial time frame. Therefore, the MS intensities at selected points over the first 24 h of the reactions are presented in Fig. 3 as ratios relative to the intensities in the corresponding thermal cracking blank from Fig. 2 (i) to allow easier comparison. The MS data for the full length of each reaction is included in the supplementary information as Figs. S7– S12.

3.2.1. Vapour-phase cracking products

At 473 K in ZSM5-FR, Fig. S7 shows that the MS signals stabilise after ca. 30 min on-stream at values which they occupy with minimal deviation for the remainder of the reaction. Compared to the baseline fragmentation pattern (Fig. 2i) the products of the reaction exhibit increased levels of fragments at 91 amu, associated with aromatic species production, and of longer chain fragments such as the hexyl (84 amu) and octyl (112 amu) ions: increased production of the octyl ion indicates the presence of alkyl chains longer than C_8 as products which fragment to give octyl ions in the mass spectrometer.

Fig. 3 (iv) shows the ZSM5-ST-473 K reaction to exhibit similar overall behaviour to that of the fresh catalyst but is less consistent across the length of the reaction (Fig. S8). Breakthrough time is reduced by approximately 50 % relative to ZSM-5-FR and, following this, the same trends in products are observed. However, rather than achieving stability, all signals begin a slow but consistent ramp back toward their baseline levels after t + 01:30 hrs. While technical difficulties prevented the following of this trend to completion, it appears that this represents a steady deactivation of the catalyst toward being unable to convert octene at 473 K.

ZSM5-FR-573 K (Fig. S9) initially produces elevated levels of saturated alkyl species, reflected in the propane contribution to the 44 amu fragment, and increased aromatic production. Levels of the octyl molecular ion indicate high conversion of the reactant. The product slate evolves significantly over the course of the reaction towards reduced production of aromatics and alkanes and increased production of olefins. The rate of all changes continues to the end of the observed reaction period. Fig. 3(v) indicates that changes in ZSM5-ST-573 K (Fig. S10) are similar to those in the fresh catalyst but less pronounced, with the exception that propane fragment levels are reduced relative to the baseline. 1-Octene conversion, as assessed by loss of the 112 amu signal, remains high throughout, although at a lower level than that observed

for ZSM5-FR-573 K.

The reactions at 673 K exhibit both the most dramatic changes *vs.* baseline, and the largest difference between the fresh and steamed zeolite catalysts. Fig. 3(iii) shows ZSM5-FR-673 K to exhibit a hundred-fold increase in aromatic production and smaller but still significant increases in the 44 and 27 amu signals. Changes in product distribution with time are slow (Fig. S11), with a slight trend toward reduction in aromatic levels and increased production of olefins. 1-Octene conversion is effectively total and remains so for the entire experimental period. In contrast, ZSM5-ST-673 K (Fig. 3 vi, Fig. S12) exhibits increased production of fragments associated with light olefins, saturated hydrocarbons, and aromatics, although aromatic production is reduced relative to the fresh catalyst. Octene conversion is lower than in the fresh catalyst and decreases over time but remains higher than achieved at lower temperatures throughout.

3.2.2. Condensable cracking products

The larger-scale reactions performed at ISIS to prepare reacted catalysts in sufficient quantity for neutron studies also produced large enough volumes of the condensable products for these to be separated and analysed. This was carried out by ATR-IR (Fig. 4).and GC-MS (Fig. 5).

At 573 K Fig. 4 shows both ZSM5-FR and ZSM5-ST produce an alkane-dominated mixture of liquids. ZSM5-FR-573 K (Fig. 4(i)(a)) contains detectable levels of aromatics, with a shoulder of the C-H stretching peaks extending above 3000 cm^{-1} and the GC-MS results (Fig. 5(i)(a)) contain peaks for mono- and di-substituted benzenes and simple naphthalenes. The IR spectrum of ZSM5-ST-573 K (Fig. 4(i)(b)) sees these features almost absent, while the GCMS results (Fig. 5(i)(b)) show a minor growth in the peaks for various cyclic isomers of the 1-octene feed, of which 1,2,3-trimethylcyclopent-1-ene is marked on Fig. 5(i)(b) as an example. Relative peak intensities in the infrared data appear similar between samples (Fig. 4(i)), suggesting that both catalysts are producing a similar mixture of alkanes at this temperature.

At 673 K ZSM5-FR produces a product slate with much higher levels of aromatic products (Fig. 5(i)(b)), including both extensively substituted benzenes and multiple naphthalene species; all of which are present in large quantities. Production of C_8 isomers is low, indicating that the catalyst favours conversion over isomerisation processes under these conditions. In contrast to the behaviour with fresh catalyst, Fig. 5 (ii)(b) shows ZSM5-ST-673 K to not produce significant quantities of bicyclic aromatics and, instead, sees an increase in rearrangement products. Levels of single-ring aromatic production are less than for the fresh catalyst at the same temperature, but higher than the fresh catalyst at 573 K.

3.3. Reacted catalyst analysis

The microreactor zeolite catalysts were retained for *ex situ* interrogation by thermogravimetric analysis (TGA) and diffuse reflectance infrared Fourier transform spectroscopy (DRIFTS). As the reactor was purged with continued gas flow following shut-off of the 1-octene supply to the reactor, these analyses provide information on those hydrocarbon species that are immobilised within the pore network. The samples were exposed to air during their removal from the microreactor, meaning that only stable species are observed. TGA allows quantification of the overall coke content of the reacted samples, given in Table 2, while the temperature at which coke oxidation occurs (Fig. 6) allow deductions to be made about the nature of that coke content. Infrared analysis by DRIFTS allows observation of the ν(C-H) and ν(O-H) regions of the sample vibrational spectra, as shown in Fig. 7. However, the region of the vibrational spectrum below 2000 cm^{-1} is dominated by modes from the zeolite framework, meaning that the deformations and C-C modes of the adsorbed hydrocarbons are largely obscured in the infrared spectra.

Table 2 shows the ZSM5-FR-473 K reaction produces a catalyst which is coked to approximately 9.5 % by weight, a level of hydrocarbon
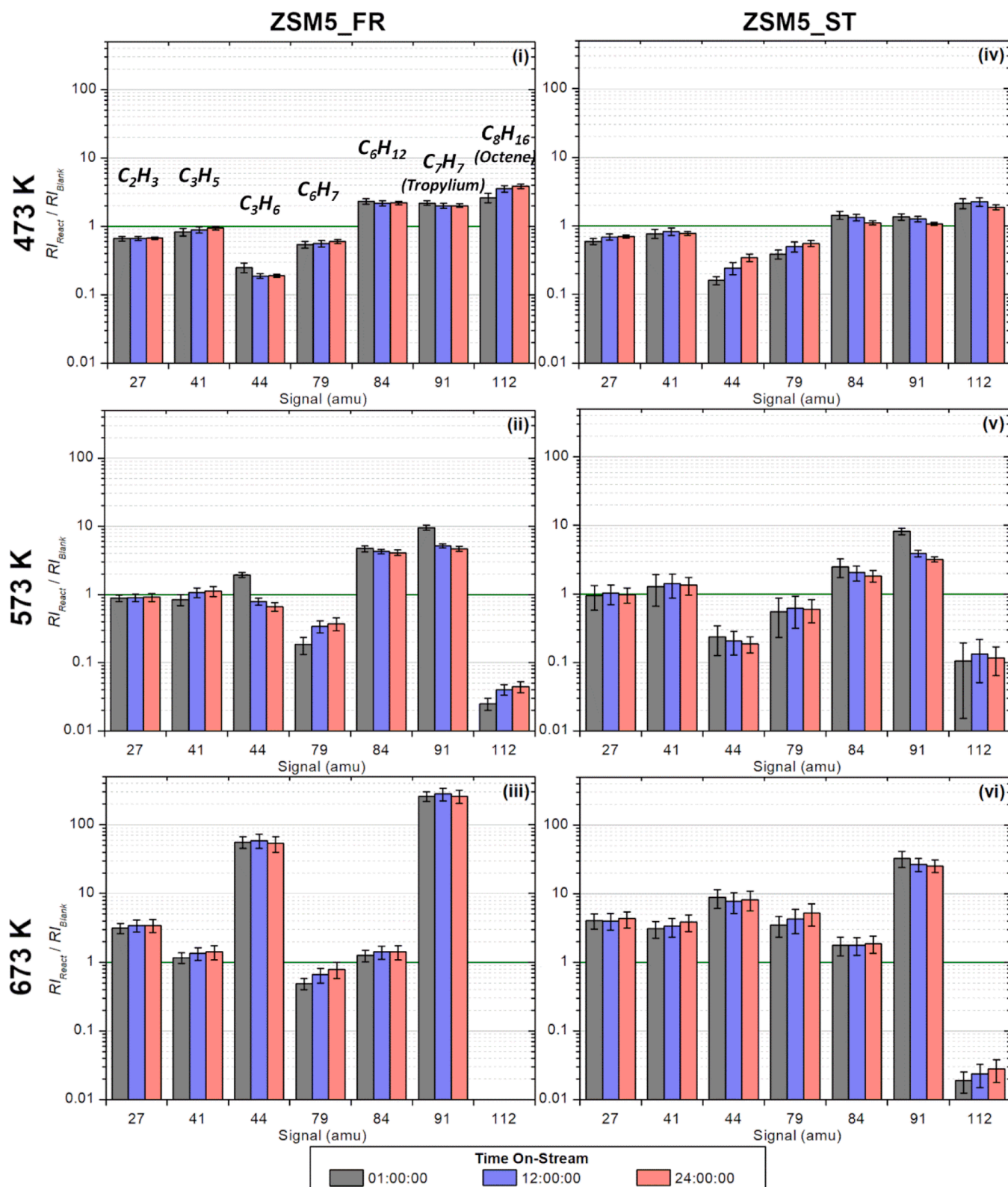
Fig. 3. Intensities of selected mass spectrum signals from the reaction of 1-octene after 1, 12 and 24 h on-stream. Reactions performed over ZSM-5-FR at 473 K (i), 573 K (ii) and 673 K (iii) and ZSM-5-ST at 473 K (iv), 573 K (v) and 673 K (vi). Fragment intensities are normalised against the signal for the reaction flow gas, averaged over ± 0.5 h from the indicated time with errors shown, and expressed as a ratio relative to the corresponding levels from thermal cracking at the same temperature (Fig. 2(i)). Thus, m/z signals above the green line have increased relative to baseline 1-octene levels, and values below the line are reduced.
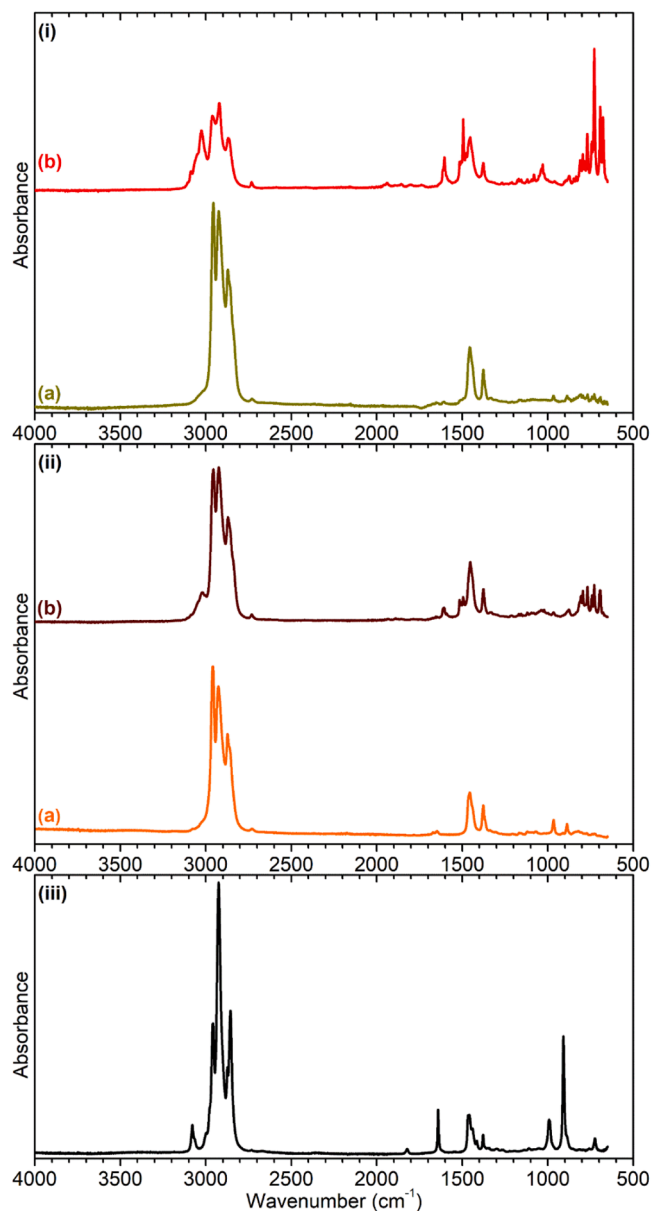
Fig. 4. Infrared spectra of the condensable product fraction from 1-octene reactions over ZSM5-FR (i) and ZSM5-ST (ii) at 573 K (a) and 673 K (b). A spectrum of pure 1-octene is included for comparison (iii). Spectra collected by ATR-IR and offset in *y*-axis.

loading which in previous studies has been found to result in the total blockage of the ZSM-5 pore structure through filling of the pore channels with hydrocarbonaceous material [33]. The majority (59 %) of this material oxidises in the range 450–650 K, which is assigned to consist of mainly saturated hydrocarbons with high hydrogen content, referred to as "Type I coke" [34].

The infrared data is consistent with this, with Fig. 7(i)(a) showing the major feature of the spectrum to be a set of peaks from 2960 to 2870 cm^{-1}, which are assigned to the symmetric and asymmetric stretches of sp^3 CH$_3$ and CH$_2$ groups [35]. The only mode attributable to unsaturated C-H stretching is the clearly separated cyclopentenyl cation peak at 3125 cm^{-1}; the corresponding asymmetric and symmetric allyl stretch modes at 1510 and 1465 cm^{-1} are also present [33,35,36]. In the O-H stretch region the intensity of the Brønsted acid peak at 3605 cm^{-1} is shifted into the broad mode from 3600 to 3400 cm^{-1}, corresponding to Brønsted OH groups weakly perturbed by adjacent coke species.

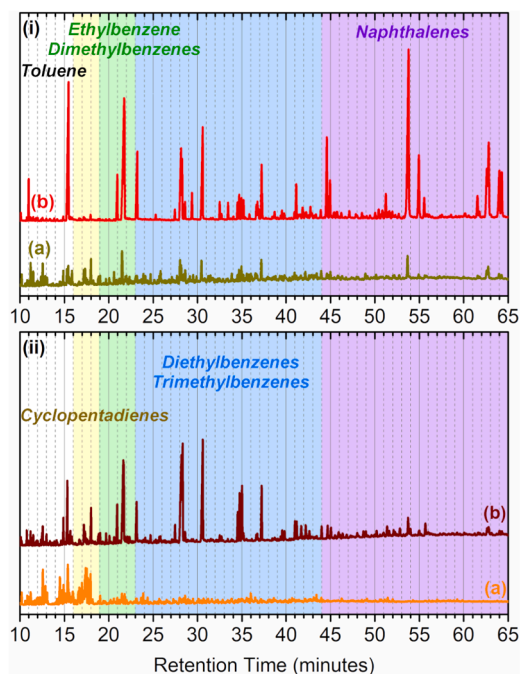The ZSM5-ST-473 K sample is approximately 7.4 % coke by weight

Fig. 5. GCMS traces of the condensable product fraction from 1-octene reactions over ZSM5-FR (i) and ZSM5-ST (ii) at 573 K (a) and 673 K (b). Retention time ranges for significant product groups are highlighted. Fig. S13

Table 2
Sample reaction times and coke content of reacted catalysts determined by thermogravimetric analysis.

Sample	Reaction Time (hrs)	Coke Content (wt%)		
		Type I	Type II	Total
ZSM5-FR-473 K	46.0	5.54	3.93	9.47
ZSM5-FR-573 K	72.0	0.58	8.70	9.28
ZSM5-FR-673 K	72.5	0.16	6.51	6.67
ZSM5-ST-473 K	24.0	6.91	0.44	7.35
ZSM5-ST-573 K	72.5	0.81	1.06	1.87
ZSM5-ST-673 K	72.0	0.14	0.64	0.78

(Table 2), similar to that of the fresh catalyst despite being reacted for only 50 % of the time on stream. The predominance of Type I coke in this material is even greater than in the fresh catalyst, with only 3.5 % of the mass loss from oxidation occurring above 650 K. In contrast to the relatively homogeneous nature of the Type I coke in ZSM5-FR-473 K, Fig. 6(ii)(a) shows the coke in the steamed catalyst to consist of two separate populations: one that oxidises around 550 K, similar to that observed in ZSM5-FR-473 K, and a second type of hydrocarbon which requires higher temperatures centred around 575 K to oxidise. The infrared spectrum (Fig. 7(ii)(a)) continues to be dominated by saturated C-H stretching modes, with the intensity of the CH$_2$-associated modes at 2930 and 2870 cm^{-1} increased relative to their methyl equivalents.

Fig. 6(i)(b) shows ZSM5-FR-573 K achieves a similar level of coke content to that observed at the lower temperature despite the differing time on-stream. However, the majority of the coke oxidises at temperatures greater than 700 K, corresponding to Type II coke consisting mainly of substituted aromatic or polyaromatic species (Table 2). This is reflected in the DRIFTS spectrum (Fig. 7(i)(b) by a significant reduction in the intensity of the sp^3 νC-H modes. However, the large quantity of Type II coke does not result in similarly significant contributions to the infrared spectrum. Peaks at 1570 and 1615 cm^{-1} in Fig. 7(i)(b) may be due to C-C stretching in mono- and di-substituted aromatic rings and are not observed at 473 K (Fig. 7(i)(a), but the only C-H stretch mode
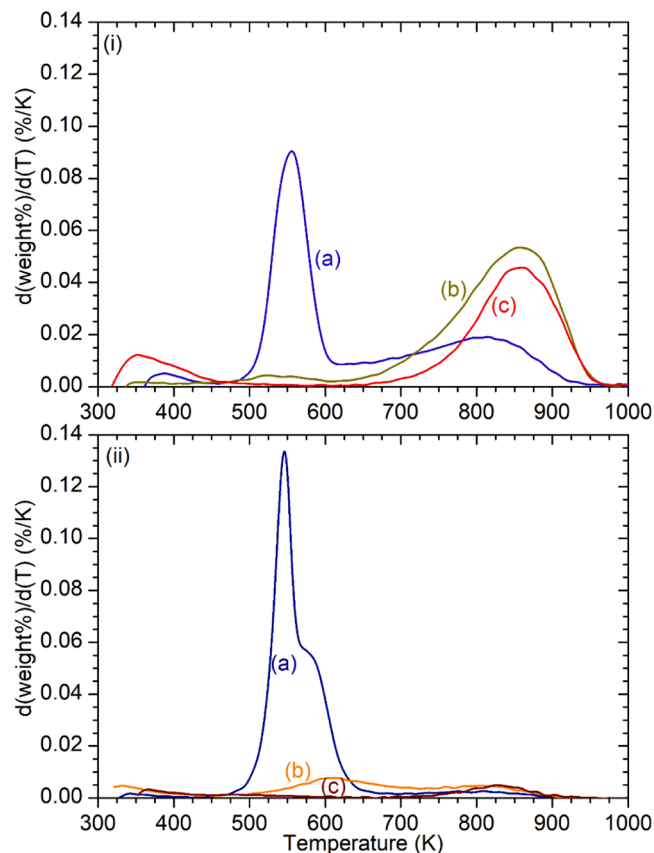
Fig. 6. Rate of weight decrease during thermogravimetric analysis in 10 % oxygen of samples of ZSM5-FR (i) and ZSM5-ST (ii) catalysts after reaction at 473 K (a), 573 K (b) and 673 K (c) showing the temperatures required for oxidation of different coke species.

Fig. 7. DRIFTS infrared spectra of samples of ZSM5-FR (i) and ZSM5-ST (ii) after reaction at 473 K (a), 573 K (b) and 673 K (c) compared with the spectrum of the catalysts pre-reaction (d). Spectra collected using DRIFTS and intensities normalised on the zeolite framework combination mode at 1870 cm^{-1} to allow direct comparison between the samples. Traces offset in *y*-axis for easier interpretation. The locations of the allyl stretching modes in cyclopentenyl cations (*) and ring stretching modes in substituted benzenes (†) are highlighted. (Figs. S13 and S14 show the same spectra overlaid to allow a direct comparison of the realtive intensities of the various species).

observed above 3000 cm^{-1} is the peak at 3125 cm^{-1} associated with cyclopentenyl cations.

The INS data collected for the repeat reactions (Fig. 8) allows much better information on the low-energy vibrational modes of the coke than is available from the DRIFTS spectra (Fig. 7) and assists in identifying the Type II coke composition. For ZSM-5-FR-573 K Fig. 8(i)(a) shows strong –CH$_3$ symmetric and antisymmetric deformations are visible at 1381 and 1452 cm^{-1}. The methylene twist located *ca.* 1300 cm^{-1} is comparatively weak, indicating that the majority of these methyl groups are not associated with alkane chains. The strong peak at 1185 cm^{-1} is associated with C-H wag modes of the ring hydrogens in aromatics and polyaromatics. However, the fact that this mode is considerably more intense than the associated modes in the 800–1100 cm^{-1} region, which are produced by hydrogens of this type in benzene and naphthalene structures, indicates that the majority of the aromatic C-H wag modes are from groups in polyaromatic structures with ≥ 3 rings, up to and including glassy carbon type materials. It is notable that the spectrum observed is extremely similar to that produced by MTH reactions at similar temperatures after extended reaction periods [37,38].

It can therefore be concluded that the coke produced on ZSM5-FR-573 K consists primarily of highly substituted aromatic and polyaromatic species with low levels of hydrogen present on sp^2 carbon atoms, leading to the infrared spectrum being dominated by the limited population of Type I coke.

In the case of ZSM5-ST-573 K, Table 2 shows this to be the first sample to have a significant difference in its level of coking, achieving only 1.9 wt% coke after 72 h. This decrease in coke loading is entirely due to a reduction in the levels of Type II coke; the quantity of Type I coke may even be increased relative to the levels in the fresh catalyst.
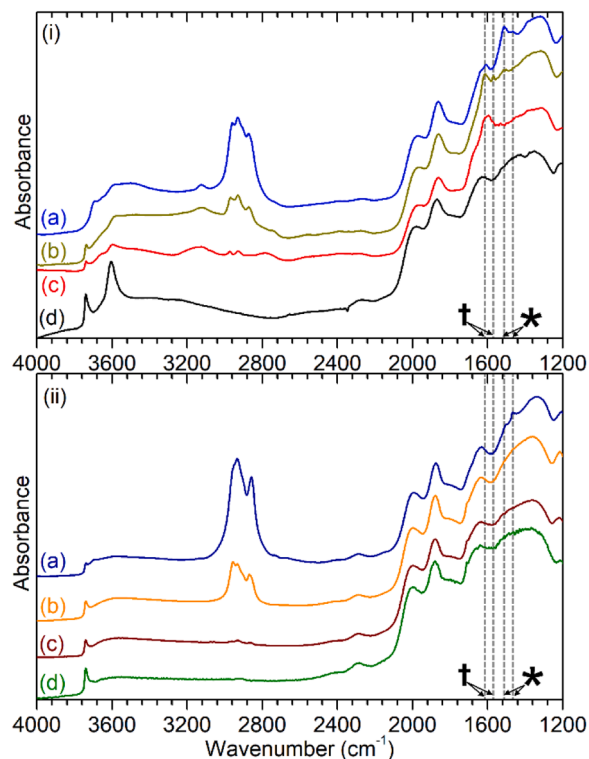
The INS spectrum confirms this (Fig. 8(ii)(a)), with ZSM5-ST-573 K returning a spectrum representative of the formation of long, linear oligomers within the zeolite, something which has been observed in several studies of octene in ZSM-5 zeolites at low temperatures [39,40]. Aromatic signals appear totally absent. Meanwhile, the relative intensity of the methylene peaks indicates that the oligomer possesses multiple CH$_2$ units but is not primarily linear due to the 720 cm^{-1} band not being significantly stronger than the other methylene modes in the 700–1100 cm^{-1} region. The infrared data also appears to support this with the intensity of the νC-H modes being increased relative to ZSM5-FR-573 K (Fig. 7(i)(b)), although the differing levels of background intensity due to greater sample darkening in ZSM5-FR-573 K make direct comparisons difficult. ZSM5-ST-573 K shows no evidence of hydrocarbon modes other than the sp^3 C-H stretches (Fig. 6(ii)(b).

The 673 K samples continue the trends observed at 573 K. ZSM5-FR-673 K sees a further reduction in Type I coke deposition to negligible levels but also sees a reduction in Type II coke build-up (Fig. 6(ii)(c)), indicating a more efficient catalytic process at this temperature. Fig. 8 (ii)(b) is consistent with this, with the spectrum of the 673 K sample having the same polyaromatic characteristics as at 573 K but at a lower overall intensity due to lower coke quantities. The infrared data shows significant reductions in all ν(C-H) modes (Fig. 7(ii)(c)), and also lower levels of evidence for adsorbed hydrocarbons in the ν(O-H) region due to the absence of immobilised coke species. Despite this, the intensity of the Brønsted and silanol O-H peaks is still reduced relative to the clean zeolite spectrum, suggesting that permanent O-H site loss is occurring.

Coke build-up in ZSM5-ST-673 K is even lower than at 573 K (Fig. 6 (ii)(c)) and is almost entirely invisible to both the infrared and the INS
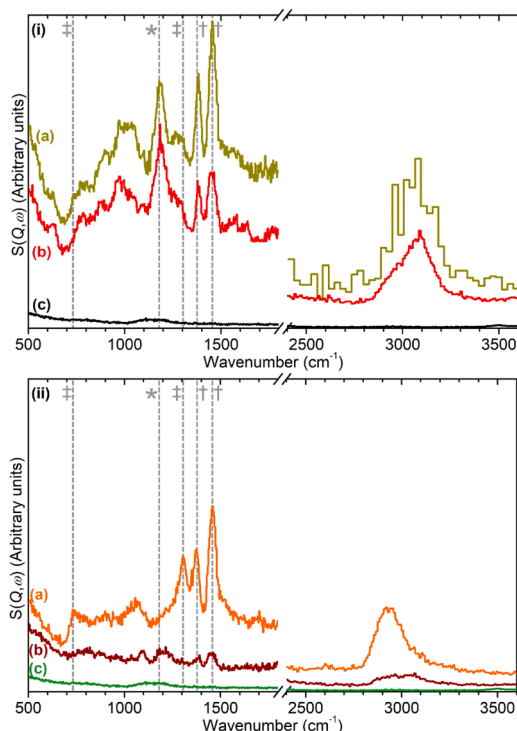
Fig. 8. INS spectra of ZSM5-FR (i) and ZSM5-ST (ii) after reaction with 1-octene at 573 K (a) and 673 K (b) compared with the spectrum of the catalysts pre-reaction (c). Modes associated with -CH$_3$ (†), -CH$_2$- (‡) and poly-aromatic (*) groups are highlighted. Spectra collected on MAPS at incident energies of 2016 (left) and 5243 (right) cm^{-1} and normalised to correct for differences in sample mass. Lower signal-to-noise ratio in high-energy spectrum (i)(a) due to shorter collection time for this sample.

analysis methods employed. This indicates that the minimal quantities of coke produced in this catalyst are almost entirely carbonaceous; the INS spectrum (Fig. 8(ii)(b) does exhibit extremely weak modes at *ca.* 1200 and 1100 cm^{-1}, corresponding to modes found in amorphous carbon samples, supporting this reasoning [41,42].

4. Discussion

4.1. The general case

The observed products of all reactions described above are consistent with the reactions within the zeolite conforming to a hydrocarbon pool type of mechanism analogous to that operating in methanol to hydrocarbons (MTH) chemistry. We have previously shown [33] that reactions of propene over H-ZSM-5 give very similar adsorbed species in the zeolite to those seen in methanol conversion. Formation of the hydrocarbon pool in MTH is considered to involve oligomerisation of initially formed light olefins, methylation by methanol, cyclisation and hydrogen transfer to form arenes and alkanes. The arenes may be further methylated or cracked to form light olefin products [43–45]. In the absence of methanol, the methylation steps involved in formation of the MTH hydrocarbon pool cannot be present. Nevertheless, early ^{13}C NMR studies by Haw et al. [46] showed that light olefins readily form oligomeric and cyclic species in H-ZSM-5 and DFT calculations have shown that cyclopentenyl species are favoured to form from olefin oligomers even in the absence of methanol. [47]. Zhang et al. [48] report that propene is much more reactive than methanol and that co-feeding methanol with propene had only a minor effect on the product stream obtained. GC-MS analysis of extracted hydrocarbons and ^{13}C NMR of used catalysts also showed evidence for cyclic species formed from propene alone.

Fig. 9 shows the dual cycle hydrocarbon pool mechanism we propose to account for the 1-octene reactions reported here. In the first cycle, protonation of 1-octene on the Brønsted acid sites of the zeolite forms bonded alkoxide species. These may subsequently undergo oligomerization to form longer chain alkyl species through further olefin addition or cracking to form shorter olefins [49,50]. In ZSM-5, due to the shape-selective effect of steric hindrance from the zeolite pore structure, the dominant mode of cracking is β-scission, to give a smaller alkoxide which remains attached to the zeolite active site and a light olefin molecule which is released into the pore network [6].

The second cycle in the hydrocarbon pool mechanism involves the production and alkylation of aromatics. Alkoxides formed in the first cycle in the C$_6$-C$_9$ length range can cyclise to form benzene, toluene or xylenes (BTX) [42,51]. The cyclisation involves cyclopentenyl species as intermediates, as proposed for MTH chemistry [43–46]. The key role of cyclopentenyl species in MTH chemistry has also prompted the suggestion [52] of a third (cyclopentenyl) cycle linking the olefin and aromatic cycles. In the absence of methanol, the hydride transfer required to form cyclopentenyl cations then aromatics will involve alkoxide species forming alkanes, as observed here.

The components of the aromatic pool can, in turn, incorporate further alkyl chains through alkylation reactions and isomerisations, allowing the production of larger substituted benzenes and poly-aromatics such as naphthalenes. Ethyl or longer side chains may be removed from an aromatic ring through an internal rearrangement and elimination to give a smaller aromatic species and a light olefin, closing the aromatic cycle and providing another source of light olefins which can re-enter either of the reaction cycles.

4.2. Reactions at 473 K

At the lowest temperature considered, the hydrocarbon pool reaction is constrained by two factors. Firstly, the rate of β-scission is temperature dependent and is therefore relatively low at this temperature. Secondly, the hydrogen transfer reaction that links the alkyl and aromatic cycles also has a very low reaction rate at 473 K [33]. The combined result of these factors is that at 473 K the cyclic component of the hydrocarbon pool mechanism is not evident, and the catalyst instead undergoes a rapid series of successive oligomerization reactions at each active site which consume all of the 1-octene supplied to the catalyst. These oligomers grow until they occupy the whole of the pore network, generating the large quantities of coke detected by TGA in ZSM5-FR-473 K (Table 2) and the strong saturated ν(C-H) modes in the infrared spectrum (Fig. 6(i) (a)). Due to the large size of the oligomer molecules, they are immobilised within the pore network and therefore act to block the catalyst active sites, resulting in ZSM5-FR-473 K being largely deactivated from early times and minimal deviation from the baseline fragmentation pattern (Fig. 3(i)). The residual reactivity is due to the minority of Brønsted sites located at the external surface of the zeolite crystallites,
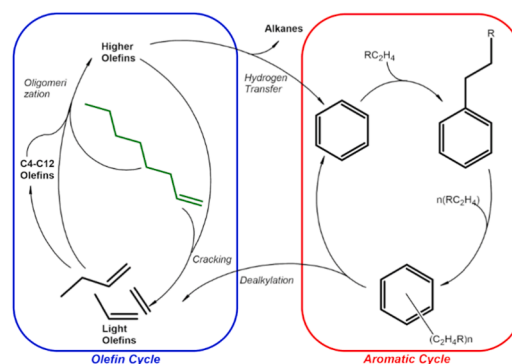

Fig. 9. Dual-cycle hydrocarbon pool mechanism for olefin reactions over ZSM-5 catalysts. [1-Column].

which are less vulnerable to blocking by immobile oligomers. The fact that cyclopentenyl ions ($m/z = 79$ amu) predominate over aromatic signals in the MS (m/z 91) (Fig. S7) is due to the hydrogen transfer reaction being the rate-limiting step in this reaction, leading to a build-up of the cyclopentenyl intermediate, which is also detectable by infrared analysis as seen in Fig. 7(i)(a). Deprotonation of the cyclopentenyl cations forms the gas phase cyclopentenyl species detected by MS. The external sites are also responsible for the production of the Type II coke which is observed by TGA (Fig. 6(i)(a)). The remaining shifts in the products after the first hour (Fig. S7) are caused by the slow deactivation of these external sites leading to progress towards a completely deactivated catalyst.

In ZSM5-ST-473 K the result is similar, however, the lower initial population of acid sites means that the time taken for the saturation of the catalyst with oligomer is lower. Despite this, the overall quantity of type I coke is comparable in both systems (Table 2) since it is the pore geometry of the zeolite which determines the amount of space available for filling by oligomer molecules and this remains largely unchanged. The wider separation of the Brønsted sites within ZSM5-ST may result in a longer average chain length for the pore blocking oligomer, as observed previously for studies of low-temperature propene oligomerisation in ZSM-5 [27]; this explains the increased intensity of CH_2 modes observed in Fig. 7(ii)(a). The separation of the Type I coke into two populations (Fig. 6(ii)(a), with one corresponding to that in the fresh catalyst and the other requiring higher temperatures to oxidise, may be due to the increased mesoporosity in the steamed zeolite (Table 1), leading to a population of larger, harder to oxidise, oligomers. The lower levels of residual production following catalyst conditioning and the more rapid decay of even this production towards a completely deactivated catalyst (Fig. S8) are explained in terms of a lower level of external, non-blocked active sites.

4.3. Reactions at 573 K

At 573 K the hydrogen transfer reactions are rapid enough for the aromatic cycle to contribute meaningfully to the overall reaction, which combined with the increased rate of β-scission means that the runaway oligomerization process does not occur in the fresh catalyst. Instead, the catalyst operates in a regime where both cycles run in equilibrium, releasing both mobile monoaromatics from the cyclisation reaction and light olefins from β-scission in the olefin cycle. The rate of production of aromatics is not stable but decays steadily with time, linked to a simultaneous decrease in 1-octene conversion, which indicates that the aromatic catalytic cycle is not fully efficient at 573 K. The deactivation is due to the catalyst coking process (Table 2), which INS indicates involves the formation of both highly substituted benzenes and naphthalenes as well as amorphous carbon-like coke species (Fig. 8(i)(a), despite the methylated aromatics not being readily apparent to infrared analysis (Fig. 7(i)(b)). This depletes the pool of aromatic hydrocarbons available for the reaction and blocks the catalytic sites suitable for the formation of fresh aromatics through cyclisation. The high coke production is likely due to the aromatic formation and alkylation reactions proceeding at a faster rate than the rearrangement and olefin elimination reactions which form the 'regeneration' arm of the aromatic cycle (Fig. 9) under the reaction conditions at 573 K. The inefficiency of the aromatic cycle may be due to slower diffusion of the aromatic products within the zeolite, leading to a high percentage of them undergoing further additions and becoming trapped. This would explain the relatively low levels of di- and tri-substituted benzenes detected by GC-MS in the liquid products (Fig. 5(i)(a)).

The progressive deactivation of the aromatic cycle leads to increased importance of the olefin-cycle, which is able to build-up a small quantity of immobile long-chain oligomers, similar to those observed at 473 K, which form the small population of Type I coke which is observed by TGA (Fig. 6(i)(b)) and INS (Fig. 8(i)(a)) and that dominates the infrared spectrum (Fig. 7(i)(b)). The catalyst is still active enough to promote

rearrangements of these oligomers during their formation, resulting in them being relatively branched with INS peaks mostly overlapping with the modes of the Type II coke.

The effect of the steam treatment is to accelerate this suppression of the aromatic cycle: peak aromatic production levels are lower and more rapidly decay toward baseline levels (Fig. 3(v)), while levels of olefin production likewise follow the distribution which would be expected from projecting the trends observed in ZSM5-FR-573 K (Fig. S9) to a timestamp considerably beyond the end of the experimental period. This reduction in aromatic cycle reactivity also has the effect of preventing the formation of polyaromatic Type II coke, meaning that catalyst deactivation occurs by the formation of large oligomers, similar to lower temperature reactions, as observed in the INS spectrum.

4.4. Reactions at 673 K

The increase in temperature to 673 K is sufficient for the restrictions to the aromatic cycle to be overcome. The level of aromatic production in ZSM5-FR-673 K (Fig. 3(iii)) is much higher than at 573 K, with aromatic signals exceeding those of released cyclopentenyl species in the MS trace for the first time (Fig. S11). Aromatic production remains stable for the first 24 h on-stream, indicating that no premature deactivation of the catalyst is occurring. This suggests that elimination reactions to remove olefins from larger aromatics can occur, recycling the aromatic ring. This supposition is supported by the significantly increased production of ethene observed due to elimination of ethyl sidechains. Some coke formation does occur (Table 2), but this takes much longer with the coke content of ZSM5-FR-673 K being only 70 % of that found in the fully coked catalysts generated at lower temperatures. That Type I coke is essentially absent from the TGA profile (Fig. 6(i)(c)) also indicates that the aromatic cycle remains active enough to prevent multiple oligomerizations until the end of the reaction run.

The effect of the steaming at this temperature is again to suppress aromatic production in favour of additional cracking and the production of light olefins, although aromatic levels are still higher than those achieved at lower temperatures. The aromatic composition is also changed, with naphthalene production being almost completely suppressed and the production of benzenes with more than two substituent groups also being significantly reduced (Fig. 5(ii)(b)). This may be due to the greater ease of diffusion in de-aluminated ZSM-5 reducing the average residence time of benzene products within the catalyst and lowering the probability of further reactions [27]. Due to the lack of opportunities for the formation of type II coke and the high rate of cracking preventing Type I coke formation, deactivation of ZSM5-ST-673 K is minor (Fig. S12), resulting in a low final coke content (Table 2) and stable product levels across the entire length of the reaction (Fig. S12).

The coke that does form at 673 K (Fig. 6(i)(c)) is similar to that generated in ZSM5-FR-573 K, with a comparable mix of mostly aromatic species. This suggests that there are two reactions within the hydrocarbon pool mechanism which have a key effect on the overall cycle chemistry: the hydrogen transfer reaction that links the alkyl and aromatic cycles and the rearrangement/elimination reactions which remove groups from pool aromatic species. Each of these reactions require successively higher temperatures to become active and deactivate as the catalyst ages and cokes. This, in turn, partitions the hydrocarbon pool into three separate reaction regimes depending on which reaction, if any, is active: (i) the fully operating catalytic cycle observed at 673 K resulting in steady-state operation with low levels of coke production; (ii) the excess polyaromatic coking regime which ZSM5-FR-673 K enters in the later stages of the reaction (and where ZSM5-FR-573 K operates throughout) and (iii) the olefin cycle only regime observed for the majority of ZSM5-ST-573 K's lifetime and for all reactions at 473 K.

5. Conclusions

The catalytic cracking reaction of 1-octene over H-ZSM-5 catalyst in the temperature range 473–673 K proceeds via a hydrocarbon pool mechanism consisting of an olefin and aromatic cycle linked by hydrogen transfer reactions. For all catalysts, the cracking products shift from a mixed aromatic-light olefins mixture, towards a purely olefinic product regime as the reaction proceeds due to coke formation blocking access to the catalytically active sites within the zeolite. The temperature of reaction determines how fast this occurs, by influencing what coke formation routes are made available by low reaction rates in key steps in the dual cycle mechanism. The use of INS allows characterisation of the retained coke species that remain within the zeolite in a way not previously realisable, assisting in the identification of two distinct deactivation mechanisms. Temperatures of 573 K or higher are necessary for the full participation of all reactions in the olefin cycle; below this temperature the catalyst is rapidly deactivated within minutes by the formation of pore-blocking alkyl species formed by multiple olefin oligomerizations. Similarly, the aromatic cycle does not operate at full efficiency below 673 K leading to excessive production of polyaromatic coke and the deactivation of the catalyst on a timescale of hours.

High temperature steam treatment of the ZSM-5 (1073 K, 12 hrs) has the effect of removing the majority of the Brønsted acidity of the zeolite through hydrothermal de-alumination of the framework without significantly affecting the zeolite's structural properties. While these conditions are somewhat removed from those used industrially (773–823 K, contact time 2–4 s), this accelerated aging of the catalyst provides an effective path to a catalyst that is more representative of the working, industrial material. The removal of these acid sites means that in ZSM5-ST the aromatic cycle is pre-emptively suppressed, and the reaction operates in the primarily light olefin producing regime from the start of the reaction, increasing the overall selectivity of the reaction towards ethene and propene. This 'Gasoline-to-Olefins' type chemistry is comparable to the results reported for ZSM-5 catalysts in industrial FCC reactors, where it is primarily used to increase the yields of propene and ethene [7,53]. The aromatic-based chemistry of the fresh catalyst is less commonly observed and is attributed to the exceptionally high acidity of ZSM5-FR.

The reduction in aromatic cycle chemistry in ZSM5-ST also has the effect of reducing the level of coke formation in the catalyst, particularly at high temperatures, by inhibiting the formation of polyaromatic Type II coke, resulting in increased stability and operating lifetime of ZSM5-ST relative to ZSM5-FR. This behaviour is similar to that observed by Ibáñez et al. [14] for the conversion of butene over mildly steamed ZSM-5. In that study, the suppression of the aromatic cycle was attributed to the selective removal of the strongest acid sites from the zeolite framework. In our case, the harsher steaming conditions employed resulted in a more complete removal of Brønsted acidity and shows no evidence of selective removal of stronger acid groups, suggesting that another mechanism may be responsible. Therefore, for octene cracking reactions catalysed by ZSM-5 zeolites both catalyst selectivity and stability are increased by steam treatment and the resulting behaviour of the treated catalyst is more representative of ZSM-5 catalysts in industrial FCC use.

CRediT authorship contribution statement

A.P. Hawkins: Methodology, Investigation, Writing – original draft, Writing – review & editing. **A. Zachariou:** Investigation, Writing – review & editing. **S.F. Parker:** Supervision, Writing – review & editing. **P. Collier:** Conceptualization, Resources, Funding acquisition. **N.S. Barrow:** Investigation. **R.F. Howe:** Supervision, Writing – review & editing. **D. Lennon:** Writing – review & editing, Project administration.

Declaration of Competing Interest

The authors declare the following financial interests/personal relationships which may be considered as potential competing interests. SF Parker, D. Lennon, A. Zachariou, AP Hawkins, RF Howe reports equipment, drugs, or supplies was provided by Johnson Matthey plc Technology Centre. P Collier, NS Barrow reports a relationship with Johnson Matthey plc Technology Centre that includes: employment.

Data availability

Data will be made available on request.

Appendix A. Supporting information

Sample details (Table S1); Assignment of mass spectra cracking patterns (Table S2); ^{27}Al solid-state NMR of fresh and steamed samples (Fig. S1); NH$_3$ TPD of fresh and steamed samples (Fig. S2); nitrogen adsorption isotherms and powder XRD of fresh and steamed samples (Fig. S3); reaction profiles (Figs. S4-S12); infrared spectra of fresh (Fig. S13) and steamed (Fig. S14) samples. Supplementary data associated with this article can be found in the online version at doi:10.1016/j.apcata.2023.119442.

References

[1] E.T.C. Vogt, B.M. Weckhuysen, Fluid catalytic cracking:recent developments on the grand old lady of zeolite catalysis, Chem. Soc. Rev. 44 (2015) 7342–7370.

[2] A. Akah, M. Al-Ghrami, Maximizing propylene production via FCC technology, Appl. Petrochem. Res. 5 (2015) 377–392.

[3] S.M. Sadrameli, Thermal/catalytic cracking of liquid hydrocarbons for the production of olefins: a state-of-the-art review II: catalytic cracking review, Fuel 173 (2016) 285–297.

[4] T.F. Degnan, G.K. Chitnis, P.H. Schipper, History of ZSM-5 fluid catalytic cracking additive development at Mobil, Microporous Mesoporous Mater. 35 (2000) 245–252.

[5] F.N. Guerzoni, J. Abbot, Cracking of an industrial feedstock over combinations of H-ZSM-5 and HY - the influence of H-ZSM-5 pretreatment, Appl. Catal. A 120 (1994) 55–69.

[6] M.A. den Hollander, M. Wissink, M. Makkee, J.A. Moulijn, Gasoline conversion: reactivity towards cracking with equilibrated FCC and ZSM-5 catalysts, Appl. Catal. A 223 (2002) 85–102.

[7] M.A. den Hollander, M. Wissink, M. Makkee, J.A. Moulijn, Synergy effects of ZSM-5 addition in fluid catalytic cracking of hydrotreated flashed distillate, Appl. Catal. A 223 (2002) 103–119.

[8] J.R. Anderson, Y.F. Chang, R.J. Western, Retained and desorbed products from reaction of 1-octene over H-ZSM-5 zeolite, Appl. Catal. 75 (1991) 87–91.

[9] Y.H. Guo, M. Pu, J.Y. Wu, J.Y. Zhang, B.H. Chen, Theoretical study of the cracking mechanisms of linear alpha-olefins catalyzed by zeolites, Appl. Surf. Sci. 254 (2007) 604–609.

[10] P.Q. Zhang, J.G. Xu, X.S. Wang, H.C. Guo, Catalytic performance of nanocrystallite HZSM-5 catalysts for transformation of normal C-8 hydrocarbons, Chin. J. Catal. 26 (2005) 216–222.

[11] L.H. Ong, M. Dömök, R. Olindo, A.C. van Veen, J.A. Lercher, Dealumination of HZSM-5 via steam-treatment, Microporous Mesoporous Mater. 164 (2012) 9–20.

[12] T.C. Hoff, R. Thilakaratne, D.W. Gardner, R.C. Brown, J.-P. Tessonnier, Thermal stability of aluminum-rich ZSM-5 zeolites and consequences on aromatization reactions, J. Phys. Chem. C 120 (2016) 20103–20113.

[13] K.S. Triantafyllidis, A.G. Vlessidis, L. Nalbandian, N.P. Evmiridis, Effect of the degree and type of the dealumination method on the structural, compositional and acidic characteristics of H-ZSM-5 zeolites, Microporous Mesoporous Mater. 47 (2001) 369–388.

[14] M. Ibáñez, E. Epelde, A.T. Aguayo, A.G. Gayubo, J. Bilbao, P. Castaño, Selective dealumination of HZSM-5 zeolite boosts propylene by modifying 1-butene cracking pathway, Appl. Catal. A 543 (2017) 1–9.

[15] A.A. Gusev, A.C. Psarras, K.S. Triantafyllidis, A.A. Lappas, P.A. Diddams, Effect of steam deactivation severity of ZSM-5 additives on LPG olefins production in the FCC process, Molecules 22 (2017) 1784.

[16] B.A. Williams, S.M. Babitz, J.T. Miller, R.Q. Snurr, H.H. Kung, The roles of acid strength and pore diffusion in the enhanced cracking activity of steamed Y zeolites, Appl. Catal. A Gen. 177 (1999) 161–175.

[17] S.M. Campbell, D.M. Bibby, J.M. Coddington, R.F. Howe, R.H. Meinhold, Dealumination of HZSM-5 zeolites: I. Calcination and hydrothermal treatment, J. Catal. 161 (1996) 338–349.

[18] S. van Donk, A.H. Janssen, J.H. Bitter, K.P. de Jong, Generation, characterization, and impact of mesopores in zeolite catalysts, Catal. Rev. 45 (2003) 297–319.

[19] L.R. Aramburo, L. Karwacki, P. Cubillas, S. Asahina, D.A.M. de Winter, M.R. Drury, I.L.C. Buurmans, E. Stavitski, D. Mores, M. Daturi, P. Bazin, P. Dumas, F. Thibault-Starzyk, J.A. Post, M.W. Anderson, O. Terasaki, B.M. Weckhuysen, The porosity, acidity, and reactivity of dealuminated zeolite ZSM-5 at the single particle level: the influence of the zeolite architecture, Chem. Eur. J. 17 (2011) 13773–13781.

[20] K. Kubo, H. Iida, S. Namba, A. Igarashi, Effect of steaming on acidity and catalytic performance of H-ZSM-5 and P/H-ZSM-5 as naphtha to olefin catalysts, Microporous Mesoporous Mater. 188 (2014) 23–29.

[21] J. Holzinger, P. Beato, L.F. Lundegaard, J. Skibsted, Distribution of aluminum over the tetrahedral sites in ZSM-5 and their evolution after steam treatment, J. Phys. Chem. C 122 (2018) 15595–15613.

[22] C.J. Heard, L. Grajciar, F. Uhlík, M. Shamzhy, M. Opanasenko, J. Čejka, P. Nachtigall, Zeolite (in)stability under aqueous or steaming conditions, Adv. Mater. 32 (2020), 2003264.

[23] A.P. Hawkins, A. Zachariou, P. Collier, R.A. Ewings, R.F. Howe, S.F. Parker, D. Lennon, Low-temperature studies of propene oligomerization in ZSM-5 by inelastic neutron scattering spectroscopy, RSC Adv. 9 (2019) 18785–18790.

[24] M. Niwa, N. Katada, New method for the temperature-programmed desorption (TPD) of ammonia experiment for characterization of zeolite acidity: a review, Chem. Rec. 13 (2013) 432–455.

[25] S. Brunauer, P.H. Emmett, E. Teller, Adsorption of gases in multimolecular layers, J. Am. Chem. Soc. 60 (1938) 309–319.

[26] J.H. de Boer, B.C. Lippens, B.G. Linsen, J.C.P. Broekhoff, A. van den Heuvel, T. J. Osinga, The *t*-curve of multimolecular N₂-adsorption, J. Colloid Interface Sci. 21 (1966) 405–414.

[27] R. Warringham, D. Bellaire, S.F. Parker, J. Taylor, R.A. Ewings, C.M. Goodway, M. Kibble, S.R. Wakefield, M. Jura, M.P. Dudman, R.P. Tooze, P.B. Webb, D. Lennon, Sample environment issues relevant to the acquisition of inelastic neutron scattering measurements of heterogeneous catalyst samples, J. Phys. Conf. Ser. 554 (2014), 012005.

[28] R.A. Ewings, J.R. Stewart, T.G. Perring, R.I. Bewley, M.D. Le, D. Raspino, D. E. Pooley, G. Škoro, S.P. Waller, D. Zacek, C.A. Smith, R.C. Riehl-Shaw, Upgrade to the MAPS neutron time-of-flight chopper spectrometer, Rev. Sci. Instrum. 90 (2019), 035110.

[29] S.F. Parker, F. Fernandez-Alonso, A.J. Ramirez-Cuesta, J. Tomkinson, S. Rudic, R. S. Pinna, G. Gorini, J.F. Castañon, Recent and future developments on TOSCA at ISIS, J. Phys. Conf. Ser. 554 (2014), 012003.

[30] S.F. Parker, D. Lennon, P.W. Albers, Vibrational spectroscopy with neutrons: a review of new directions, Appl. Spectrosc. 65 (2011) 1325–1341.

[31] N. Malicki, G. Mali, A.-A. Quoineaud, P. Bourges, L.J. Simon, F. Thibault-Starzyk, C. Fernandez, Aluminium triplets in dealuminated zeolites detected by ²⁷Al NMR correlation spectroscopy, Microporous Mesoporous Mater. 129 (2010) 100–105.

[32] A.P. Hawkins, A. Zachariou, S.F. Parker, P. Collier, R.F. Howe, D. Lennon, Effect of steam de-alumination on the interactions of propene with H-ZSM-5 zeolites, RSC Adv. 10 (2020) 23136–23147.

[33] A.P. Hawkins, A. Zachariou, S.F. Parker, P. Collier, R.F. Howe, D. Lennon, Studies of propene conversion over H-ZSM-5 demonstrate the importance of propene as an intermediate in methanol-to-hydrocarbons chemistry, Catal. Sci. Technol. 11 (2021) 2924–2938.

[34] S. Müller, Y. Liu, M. Vishnuvarthan, X. Sun, A.C. van Veen, G.L. Haller, M. Sanchez-Sanchez, J.A. Lercher, Coke formation and deactivation pathways on H-ZSM-5 in the conversion of methanol to olefins, J. Catal. 325 (2015) 48–59.

[35] D. Lin-Vien, N.B. Colthup, W.G. Fateley, J.G. Grasselli, The Handbook of Infrared and Raman Characteristic Frequencies of Organic Molecules, Academic Press, 1991.

[36] I.B. Minova, S.K. Matam, A. Greenaway, C.R.A. Catlow, M.D. Frogley, G. Cinque, P. A. Wright, R.F. Howe, Elementary steps in the formation of hydrocarbons from surface methoxy groups in HZSM-5 seen by synchrotron infrared microspectroscopy, ACS Catal. 9 (2019) 6564–6570.

[37] A. Zachariou, A.P. Hawkins, S.F. Parker, D. Lennon, R.F. Howe, Neutron spectroscopy studies of methanol to hydrocarbons catalysis over ZSM-5, Catal. Today 368 (2020) 20–27.

[38] A. Zachariou, A.P. Hawkins, Suwardiyanto, P. Collier, N. Barrow, R.F. Howe, S. F. Parker, D. Lennon, New spectroscopic insight into the deactivation of a ZSM-5 methanol-to-hydrocarbons catalyst, ChemCatChem 13 (2021) 2625.

[39] C.S.H. Chen, R.F. Bridger, Shape-selective oligomerization of alkenes to near-linear hydrocarbons by zeolite catalysis, J. Catal. 161 (1996) 687–693.

[40] A.P. Hawkins, A.J. O'Malley, A. Zachariou, P. Collier, R.A. Ewings, I.P. Silverwood, R.F. Howe, S.F. Parker, D. Lennon, Investigation of the dynamics of 1-octene adsorption at 293 K in a ZSM-5 catalyst by inelastic and quasielastic neutron scattering, J. Phys. Chem. C 123 (2018) 417–425.

[41] A.N. Mlinar, P.M. Zimmerman, F.E. Celik, M. Head-Gordon, A.T. Bell, Effects of Brønsted-acid site proximity on the oligomerization of propene in H-MFI, J. Catal. 288 (2012) 65–73.

[42] J.F. Haw, D.M. Marcus, Well-defined (supra)molecular structures in zeolite methanol-to-olefin catalysis, Top. Catal. 34 (2005) 41–48.

[43] U. Olsbye, S. Svelle, K.P. Lillerud, Z.H. Wei, Y.Y. Chen, J.F. Li, J.G. Wang, W.B. Fan, The formation and degradation of active species during methanol conversion over protonated zeotype catalysts, Chem. Soc. Rev. 44 (2015) 7155–7176.

[44] H. Schulz, About the mechanism of methanol conversion on zeolites, Catal. Lett. 148 (2018) 1263–1280.

[45] A. Hwang, A. Bhan, Deactivation of zeolites and zeotypes in methanol-to-hydrocarbons catalysis: mechanisms and circumvention, Acc. Chem. Res. 52 (2019) 2647–2656.

[46] J.F. Haw, J.B. Nicholas, F. Song, W. Deng, F. Wang, T. Xu, C.S. Heneghan, Roles for cyclopentenyl cations in the synthesis of hydrocarbons from methanol on zeolite catalyst H-ZSM-5, J. Am. Chem. Soc. 122 (2000) 4763–4775.

[47] S. Wang, Y. Chen, Z. Qin, T.-S. Zhao, S. Fan, M. Dong, J. Li, W. Fan, J. Wang, Origin and evolution of the initial hydrocarbon pool intermediates in the transition period for the conversion of methanol to olefins over H-ZSM-5 Zeolite, J. Catal. 369 (2019) 382–395.

[48] L. Zhang, S. Wang, Z. Qin, P. Wang, G. Wang, M. Dong, W. Fan, J. Wang, Probing into the building and evolution of primary hydrocarbon pool species in the process of methanol to olefins over H-ZSM-5 zeolite, Mol. Catal. 516 (2021), 111968.

[49] G. Spoto, S. Bordiga, G. Ricchiardi, D. Scarano, A. Zecchina, E. Borello, IR study of ethene and propene oligomerization on H-ZSM-5: hydrogen-bonded precursor formation, initiation and propagation mechanisms and structure of the entrapped oligomers, J. Chem. Soc. Faraday Trans. 90 (1994) 2827–2835.

[50] F. Geobaldo, G. Spoto, S. Bordiga, C. Lamberti, A. Zecchina, Propene oligomerization on H-mordenite: hydrogen-bonding interaction, chain initiation, propagation and hydrogen transfer studied by temperature-programmed FTIR and UV–VIS spectroscopies, J. Chem. Soc. Faraday Trans. 93 (1997) 1243–1249.

[51] M. Vandichel, D. Lesthaeghe, J.V. d Mynsbrugge, M. Waroquier, V. Van Speybroeck, Assembly of cyclic hydrocarbons from ethene and propene in acid zeolite catalysis to produce active catalytic sites for MTO conversion, J. Catal. 271 (2010) 67–78.

[52] W. Zhang, Y. Zhi, J. Huang, X. Wu, S. Zeng, S. Xu, A. Zheng, Y. Wei, Z. Liu, Methanol to olefins reaction route based on methylcyclopentadienes as critical intermediates, ACS Catal. 9 (2019) 7373–7379.

[53] O. Awayssa, N. Al-Yassir, A. Aitani, S. Al-Khattaf, Modified HZSM-5 as FCC additive for enhancing light olefins yield from catalytic cracking of VGO, Appl. Catal. A 477 (2014) 172–183.

[54] D. Lennon, S.F. Parker, A. Zachariou, A.P. Hawkins, P. Collier, R.F. Howe, Reactions of 1-octene over H-ZSM-5: a model system for fluidised catalytic cracking, STFC ISIS Neutron Muon Source Exp. (2020), https://doi.org/10.5826/ISIS.E.RB2002126.

[55] D. Lennon, S.F. Parker, A.P. Hawkins, A. Zachariou, Towards an improved understanding of the interaction of methanol over zeolite catalysts, STFC ISIS Neutron Muon Source Exp. (2020), https://doi.org/10.5286/ISIS.E.RB201048.